

Research on SVG Control Method Under Unbalanced Conditions

Zheng Zheng, Yousong Zhou*, Guopeng Zhang

School of Electrical Engineering and Automation, Henan Polytechnic University
Jiaozuo, 454000, China

E-mail: zhengzh@hpu.edu.cn, z2410767638@163.com, hpoyz@163.com

http://www.hpu.edu.cn/www/index.html

Abstract

In order to reduce the complexity of traditional methods, a PCI (Proportional Complex Integral) controller is adopted to control SVG under unbalance-grid condition, which has better performance than PI controller to eliminate steady-state error to compensate nonlinear loads. Based on the $\alpha\beta$ frame, the proposed control scheme considerably reduces total algorithm complexity. The current control loop is designed based on mathematical modeling under unbalanced conditions. Simulation and experimental results are provided to validate the correctness of the proposed methods.

Keywords: SVG; complex filter; steady-state error; proportional complex integral control;

1. Introduction

In recent years, the research of SVG (Static Var Generator) is mainly focused on the fast and accurate detection of reactive current component and the simplification of reactive power control methods^{1,2}. Proportional-resonant control method³⁻⁴ can make the input current achieve the zero steady state error. However, the method has a high requirement for the accuracy of the equipment parameters, which is difficult to achieve the ideal state. Deadbeat control method and predictive current control method are used in paper⁵⁻⁷. These control methods have some difficulties in the design of precise models, which can easily cause the system to appear unstable.

This paper presents PCI control method based on $\alpha\beta$ stationary reference frame. The control method not only effectively eliminates the steady-state error of AC current, but also improves the compensation performance of the equipment.

2. Control Method

The main circuit structure of the voltage-source SVG is shown in Fig.1. Phase voltage of three-phase power grid is expressed as e_a, e_b and e_c ; Three-phase load current is represented by i_{la}, i_{lb} and i_{lc} ; The DC side voltage is expressed as u_{dc} .

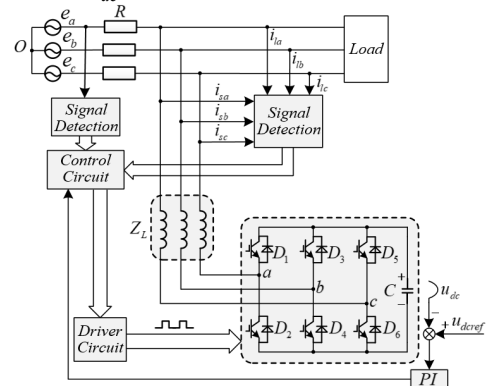


Fig.1. Main circuit topology of SVG

*Corresponding author

2.1. Positive and negative component separation method based on complex filter

In this paper, a method of separating positive/negative sequence components from the grid current by using the complex filter is proposed. The principle block diagram is shown in Fig.2. In figure, ω_c is the cut-off frequency of the filter.

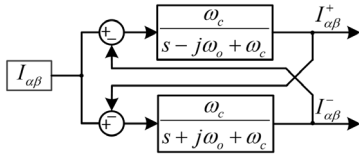


Fig.2. Separation of the positive/negative sequence current

From Fig.2, $I_{\alpha\beta}^+(s)$ and $|F(s)|$ can be achieved as:

$$I_{\alpha\beta}^+(s) = \frac{\omega_c (s + j\omega_o)}{s^2 + 2\omega_c s + \omega_o^2} I_{\alpha\beta}(s) = F(s) I_{\alpha\beta}(s) \quad (1)$$

$$|F(s)| = \frac{|\omega_c (\omega + \omega_o)|}{\sqrt{(\omega_o^2 - \omega^2)^2 + 4\omega_c^2 \omega^2}} \quad (2)$$

Three-phase current transformed into $\alpha\beta$ stationary coordinate system can be written as:

$$\begin{bmatrix} I_\alpha \\ I_\beta \end{bmatrix} = \frac{2}{3} \begin{bmatrix} 1 & -\frac{1}{2} & \frac{1}{2} \\ 0 & \frac{\sqrt{3}}{2} & -\frac{\sqrt{3}}{2} \end{bmatrix} \begin{bmatrix} I_a \\ I_b \\ I_c \end{bmatrix} = \begin{bmatrix} I_\alpha^+ + I_\alpha^- \\ I_\beta^+ + I_\beta^- \end{bmatrix} \quad (3)$$

A specific block diagram is shown in Fig.3.

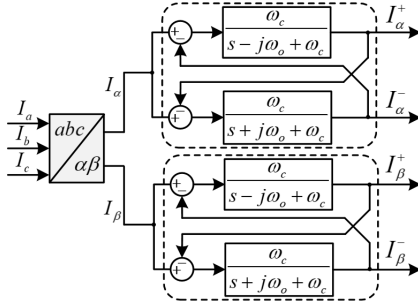


Fig.3. Separation of positive/negative sequence current under three-phase unbalance

2.2. PCI control method

The traditional proportional complex integral control is based on $\alpha\beta$ stationary coordinate system as shown in Fig.4. When the current is controlled in three-phase coordinate system, the control computation is greatly increased due to the coordinate transformation. In this paper, according to the equivalent transformation of

variables, proportional complex integral control which can be applied directly in three-phase coordinate system is designed.

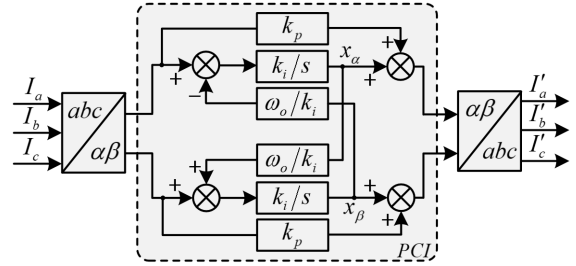


Fig.4. PCI control based on $\alpha\beta$ stationary coordinate system

The phase difference of each phase is 120° , which can be given as

$$\begin{cases} -j\sqrt{3}x_a = x_b - x_c \\ -j\sqrt{3}x_b = x_c - x_a \\ -j\sqrt{3}x_c = x_a - x_b \end{cases} \quad (4)$$

The control diagram of three-phase orthogonal frame from (4) is shown in Fig.5.

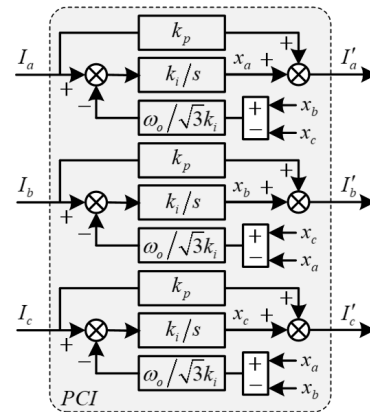


Fig.5. PCI control based on three-phase orthogonal frame

3. Analysis of simulation result

The relevant system parameters are given in Table 1.

Table 1. System Parameters

Parameter	Value	Parameter	Value
Grid Line Voltage	400V	DC side voltage	700V
Grid Frequency	50Hz	DC bus capacitor	6μF
Grid Reactance	5mH	The rated Capacity	200kVar

In the system, the bandwidth is usually selected to be 10 times higher than the fundamental frequency, and also less than 1/5 of the switching frequency, so the

range of bandwidth f_b is 500 to 2000. The transfer function of the closed loop of the system is obtained as

$$T(s) = \frac{I_o(s)}{I_r(s)} = \frac{K(k_p s + k_i - j\omega_o k_p)}{Ls^2 + (Kk_p + R - j\omega_o L)s + Kk_i - j\omega_o(Kk_p + R)} \quad (5)$$

$$|T(s)| = \frac{K\sqrt{k_p^2(\omega - \omega_o)^2 + k_i^2}}{\sqrt{(L\omega\omega_o - L\omega^2 + Kk_i)^2 + (Kk_p + R)^2(\omega - \omega_o)^2}} \quad (6)$$

$$\angle T(s) = \arctan\left(\frac{k_p(\omega - \omega_o)}{k_i}\right) - \arctan\left(\frac{(Kk_p + R)(\omega - \omega_o)}{L\omega\omega_o - L\omega^2 + Kk_i}\right) \quad (7)$$

When only k_p is considered, the closed loop amplitude frequency features can be achieved as

$$|T(s)| = \frac{Kk_p}{\sqrt{(L\omega^2)^2 + (Kk_p + R)^2}} \quad (8)$$

Where $f_b=650\text{Hz}$, $\omega_b=4100\text{rad/s}$, (8) give rises to $k_p=0.1$. Under the requirements of the system bandwidth, the design make $f_b=690\text{Hz}$, $\omega_b=4330\text{rad/s}$, (6) give rises to $k_p=20$. Under unbalanced conditions, the SVG control strategy based on complex filter and PCI control can be shown in Fig. 6.

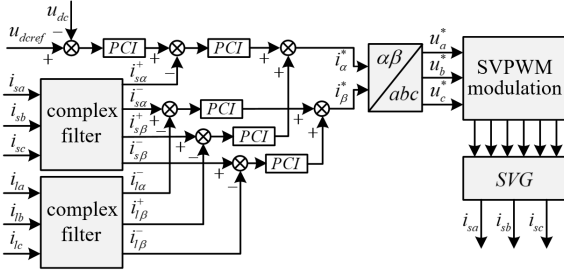


Fig. 6. The Model of SVG

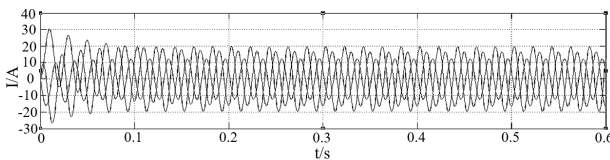


Fig.7. (a) The load current

According to above model, simulation is carried out in MATLAB/Simulink environment. Fig.7 shows the load current. Fig.8 shows tracking error comparison of the output current between PI control and PCI control. When the system is controlled under PCI control after 0.5s, the SVG output current is close to reference current, and the error is controlled to 0.1A. So PCI control has a good effect on steady state error.

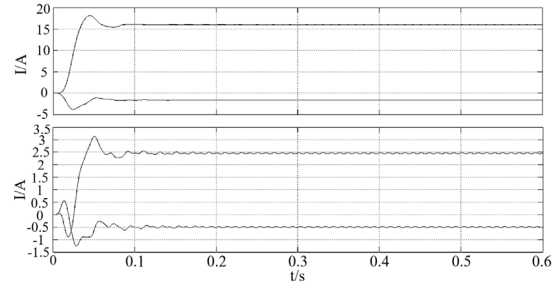


Fig.7. (b) Positive and negative sequence component of load current

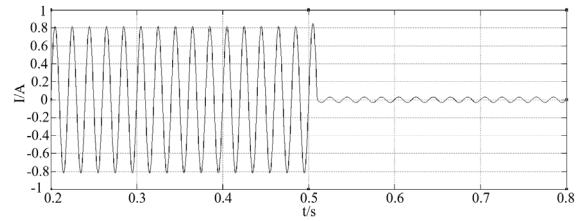


Fig. 8. Tracking error comparison of the output current between PI control and PCI control

4. Experimental Verification

In this paper, RT-LAB semi-physical platform is verified to the proposed strategy as shown in Fig. 9. The SVG control circuit is based on the core of DSP28335, and the main part of the circuit is realized by the RT-LAB platform. For the system, the phase voltage value of input grid is 311V, the DC side voltage is 700V, and the resistance of pure resistive load is 100 Ω.

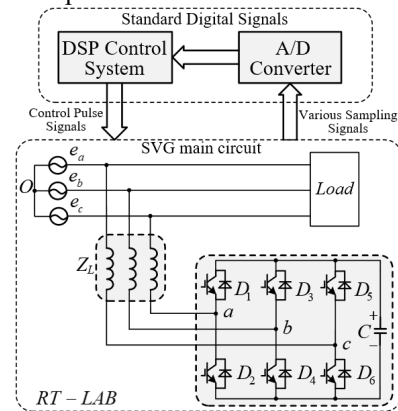


Fig.9. Schematic diagram of system structure

In order to avoid the disturbance caused by the equipment start-up, the equipment is cut off after the normal running time of 1s, and the experimental

waveforms of this system are shown in Fig. 10, Fig. 11 and Fig. 12.

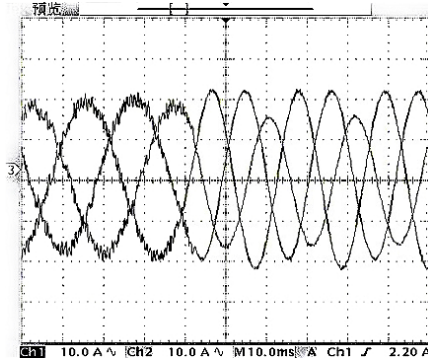


Fig. 10. Three-phase current on grid side

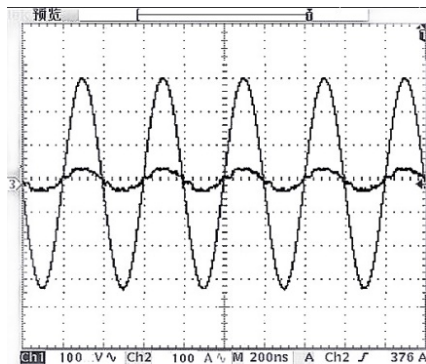


Fig. 11. Voltage and current of A grid phase

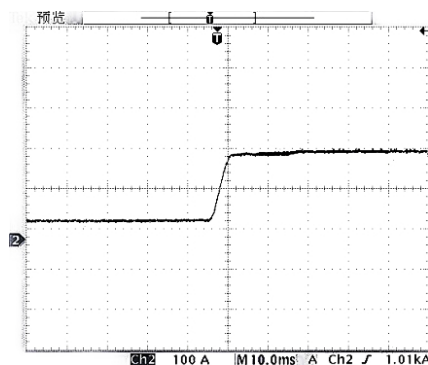


Fig. 12. Three-phase load current unbalance

Fig.10 shows three-phase current state can be balanced when the device is operating normally; while the device is disconnected, the system state becomes unbalanced. As shown in Fig.11, after compensating for reactive component and negative component, the voltage of A phase is in accordance with the phase angle of this phasic current, which reveals that the system has

better compensation effect. From Fig.12, it can be seen that unbalance degree is reduced from 0.28 to 0.06 for the three phase current of the load, which achieve the state's demand for unbalance degree.

The experimental results show that the SVG control strategy based on complex filter and PCI control can realize real-time compensation for reactive component and negative component under unbalanced conditions.

5. Conclusion

Under unbalanced condition, the PCI controller is studied using in SVG to compensate nonlinear loads. Compared with traditional control method, the proposed scheme can considerably reduce total algorithm complexity. The current control loop is designed based on the mathematical modeling under unbalanced input conditions, and parameters of PCI controller is designed. An experimental platform is built based on DSP 28335 and RT-Lab. Simulation and experimental results are given to demonstrate the effectiveness of the proposed control scheme.

Acknowledgements

Fund projects: National Natural Science Foundation (U1504518).

References

1. Y. Liu and C. Shao, Reconstruction strategies for phase currents in three phase voltage source PWM inverters, *J. Inf. Contr.* **36**(4), 2007, pp.506-513.
2. Y.N.Yu, R.F. Yang, et al. Attractive beat control of cascaded H-bridge SVG, *J. Trans. China Electrotechnical Soc.* **01**(25), 2017, pp. 50-58.
3. L. Ma, X.M. Jin, et al. Analysis of three-phase grid-connected inverter proportional resonant control and grid voltage feed-forward, *J. Trans. China Electrotechnical Soc.* **08**(27), 2012, pp. 56-62.
4. S.Bhowmik, R.Spec, J.Enslin. Performance optimization for doubly-fed wind power generation systems. *J. IEEE Trans. Ind. Appl.*, 1999, pp. 2387-2394.
5. X.G. Zhang, R.Wang and D.G. XU. A dead-beat control strategy for circulating-current in parallel connection systems of three-phase PWM converters, *J. Proc. CSEE*, **02**(33), 2013, pp. 31-37.
6. Z.J.Fang, S.X. Duan, et al. Formation mechanism and suppression strategy of prediction control error applied in a battery energy storage inverter, *J. Proc. CSEE*, **10**(30), 2013, pp. 1-9.
7. W. Chen and J. Wu. Adaptive control of ASVG by using diagonal recurrent neural network, *J. Proc. CSU-EPSSA*, 1999, pp. 33-37.